

## ORIGINAL ARTICLE

# Magnetic Resonance Imaging Texture Analysis in the Detection of Metastatic Lymph Nodes in Patients with Nasopharyngeal Carcinoma

## Nazofarenks Karsinomu Olan Hastalarda Metastatik Lenf Nodlarının Saptanmasında Manyetik Rezonans Görüntüleme Doku Analizi

<sup>1</sup>Halil Özer , <sup>2</sup>Abdussamet Batur , <sup>1</sup>Nurullah Özdemir , <sup>1</sup>Mehmet Sedat Durmaz , <sup>1</sup>Abidin Kılınçer 

<sup>1</sup>Department of Radiology, Selçuk University School of Medicine, 42131, Konya, Turkey

<sup>2</sup>Department of Radiology, Mardin Artuklu University School of Medicine, 47200, Mardin, Turkey

## Correspondence

Halil Özer, Department of Radiology, Selçuk University School of Medicine, 42131, Konya, Turkey

E-Mail: [drhalilozer@gmail.com](mailto:drhalilozer@gmail.com)

## How to cite ?

Özer H. , Batur A. , Özdemir N. , Durmaz M. S. , Kılınçer A. Magnetic Resonance Imaging Texture Analysis in the Detection of Metastatic Lymph Nodes in Patients with Nasopharyngeal Carcinoma. Genel Tıp Dergisi. 2023; 33(4): 461-465.

## ABSTRACT

**Aims:** To investigate the role of magnetic resonance imaging (MRI) texture analysis (TA) in the detection of metastatic lymph nodes in patients with nasopharyngeal carcinoma (NPC).

**Material and methods:** Between January 2020 and October 2021, 15 NPC patients with 32 metastatic lymph nodes and 30 healthy subjects with benign lymph nodes were included in the study. The texture features compared between metastatic and benign lymph nodes. The independent predictor parameters of metastatic lymph nodes were determined using multivariate regression analysis. Receiver operator characteristics (ROC) analysis was used to evaluate the diagnostic performance of the regression models.

**Results:** The first order texture features did not differ significantly between groups ( $p>0.05$ ). Except for correlation in metastatic lymph nodes, all gray-level co-occurrence matrix (GLCM) and gray-level run length matrix (GLRLM) features were significantly different ( $p<0.05$ ). The GLCM features of joint entropy, joint energy, and maximum probability; and the GLRLM features of gray level non uniformity and low gray level run emphasis were independent predictors of metastatic lymph nodes. The area under the curve (AUC) values for the GLCM regression model and GLRLM regression model were 0.975 and 0.928, respectively.

**Conclusion:** MRI texture analysis may be useful to detect metastatic lymph nodes in patients with NPC by providing quantitative information on tissue heterogeneity and cellular composition.

**Key words:** Magnetic resonance imaging, texture analysis, nasopharyngeal carcinoma, metastatic lymph nodes

## ÖZ

**Amaç:** Nazofarenks karsinomu (NK) olan hastalarda metastatik lenf nodlarının saptanmasında manyetik rezonans görüntüleme (MRG) doku analizinin (DA) rolünü araştırmak.

**Gereç ve yöntemler:** Ocak 2020-Ekim 2021 tarihleri arasında 32 metastatik lenf nodu olan 15 NK hastası ve benign lenf nodu olan 30 sağlıklı birey çalışmaya dahil edildi. Doku özellikleri, metastatik ve benign lenf nodları arasında karşılaştırıldı. Çok değişkenli regresyon analizi kullanılarak metastatik lenf nodlarını tahmin için bağımsız değişkenler belirlendi. Regresyon modellerinin tanılabilir performansını değerlendirmek için receiver operator characteristics (ROC) analizi kullanıldı.

**Bulgular:** First order doku özellikleri grupları arasında anlamlı farklılık göstermedi ( $p>0.05$ ). Metastatik lenf nodlarındaki correlation dışında tüm gray-level co-occurrence matrix (GLCM) ve gray-level run length matrix (GLRLM) özellikleri anlamlı olarak farklıydı ( $p<0.05$ ). GLCM özelliklerinden joint entropy, joint energy ve maximum probability; GLRLM özelliklerinden gray level non uniformity ve low gray level run emphasis metastatik lenf nodlarının tahmininde bağımsız değişkenlerdi. GLCM regresyon modeli ve GLRLM regresyon modeli için eğri altındaki alan (AUC) değerleri sırasıyla 0,975 ve 0,928 idi.

**Sonuç:** MRG doku analizi, doku heterojenitesi ve hücresel kompozisyon hakkında kantitatif bilgi sağlayarak NK'li hastalarda metastatik lenf nodlarını saptamada yararlı olabilir.

**Anahtar kelimeler:** Manyetik rezonans görüntüleme, doku analizi, nazofarenks karsinomu, metastatik lenf nodları

## Introduction

Nasopharyngeal carcinoma (NPC) is a highly aggressive tumor that develops from the epithelial cells of the nasopharynx (1). Nasopharyngeal tumors initially develop without producing any signs and symptoms as a result of location and the anatomical structure of the nasopharynx (1, 2). Lymphatic spread is a common feature of NPC, and accurate lymph node status assessment is critical for determining disease extent and optimizing treatment strategies (1, 3). Magnetic resonance imaging (MRI) has emerged as a valuable diagnostic tool in local staging and diagnosis of lymph nodes associated with NPC (2, 4). Metastatic lymph nodes frequently exhibit distinctive

imaging findings, such as size, shape, and internal structure (2, 5, 6). Size is an important criterion for distinguishing metastatic lymph nodes, although it alone is not definitive. The short axis of the lymph node in the axial plane is greater than 10 mm ( $\geq 11$  mm for level 2,  $\geq 5$  mm for retropharyngeal) suggests lymph node metastasis (4-6). Morphological assessment is also essential as metastatic nodes tend to have more rounded shapes, loss of fatty hilum, presence of necrosis or cystic component, and poorly defined margins (5-8). Moreover, metastatic nodes frequently exhibit high signal intensity on T2-weighted images, as well as avid heterogeneous contrast enhancement

due to increased vascularity and neovascularization (2, 9). However, since metastatic cells may be found in small and ovoid lymph nodes, morphological evaluation may be insufficient (5).

Texture analysis (TA) is a quantitative image analysis method that examines the distribution and connectivity of pixel intensities inside normal and diseased tissues to assess signal heterogeneity (10, 11). Studies have demonstrated the potential utility of TA as a noninvasive method for the differential diagnosis of NPC, assessment of NPC treatment response, and identification of metastatic lymph nodes in the head and neck region. (11-16). The purpose of this study is to investigate the role of magnetic resonance imaging texture analysis in the detection of metastatic lymph nodes in NPC.

### Material and Methods

The study was approved by our hospital's institutional ethics committee (2023/295), and the requirement for written informed consent was waived.

#### Patients

Between January 2020 and October 2021, 18 patients with a diagnosis of NPC who underwent MRI for staging were evaluated retrospectively. The diagnosis of NPC was confirmed histopathologically. The radiological criteria were used to evaluate the metastatic lymph nodes. The radiological criteria for metastatic lymph nodes were as follows: (1) In the axial plane, short-axis diameter is  $\geq 10$  mm ( $\geq 11$  mm in level II and  $\geq 5$  mm in the retropharyngeal group); (2) Lymph nodes with a round shape (long axis to short axis ratio  $< 2$ ); (3) necrotic or cystic lymph nodes; (4) evidence of extra nodal extension. The study included metastatic lymph nodes with a short axis greater than 10 mm and no cystic or necrotic components in patients with biopsy proven NPC and underwent MRI. The three largest metastatic lymph nodes in patients with multiple nodes were examined. Patients with poor image quality ( $n=1$ ) and a history of prior radio-chemotherapy ( $n=2$ ) were excluded from the study. Finally, the study included 15 consecutive cases with 32 metastatic lymph nodes.

The study included 30 healthy subjects with no history of primary malignant disease who underwent neck MRI examination for different indications as the control group. For the normal lymph node, the following criteria were used: (1) Ovoid and regular shape; (2) preserved fatty hilum; (3) short axis less than 10 mm.

#### Imaging Protocol

MRI examinations were performed using 1.5 T (MAGNETOM Area; Siemens Healthineers AG, Erlangen, Germany) scanner and 3T scanner (MAGNETOM Skyra; Siemens Healthineers AG, Erlangen, Germany). Our hospital's routine neck MRI protocol was used to scan the patients as follows: (1) axial T2-weighted imaging (WI) with fat-suppression; (2) coronal T2-WI with fat-suppression; (3) sagittal T2-WI; (4) axial T1-WI with and without fat-suppression; (5) coronal T1-WI; (6) diffusion weighted imaging (DWI) with b-values

of 0 and 800 s/mm<sup>2</sup>; (7) contrast-enhanced axial T1WI with and without fat-suppression; (8) contrast-enhanced coronal T1WI. As a contrast agent, all patients received intravenous gadoterate meglumine (Dotarem, Guerbet) and gadobutrol (Gadovist, Bayer) per kilogram of body weight.

#### Image Analysis

Two radiologists with six and three years of experience in head and neck imaging, respectively, and an awareness of all clinical and histopathological findings, interpreted the MRI in consensus. Metastatic and benign lymph nodes were identified at dedicated workstations according to inclusion criteria. For segmentation and TA, all images were imported into a commercially available program (Olea Sphere® 3.0, Olea Medical, La Ciotat, France). The normalization of the MRI exam of different scanners was done automatically by the software program. The region of interest (ROI) was created using the freehand technique that covered the whole lesion on the post contrast T1WI. To eliminate the partial volume averaging effect, the center of the lymph node whose continuity was observed in consecutive sections was selected. For each ROI, 41 texture features were extracted. The texture features included first-order parameters, gray-level co-occurrence matrix (GLCM), and gray-level run length matrix (GLRLM).

#### Statistical Analysis

The Statistical Package for the Social Sciences (SPSS), version 21.0, developed by IBM Corporation in Armonk, NY, USA, was utilized for data analysis. The normality of the distribution of continuous numerical variables was determined using the Shapiro-Wilk test. Descriptive statistics were presented as the mean and standard deviation (SD) or median (range) for continuous numerical variables, and as count and percentage for categorical variables.

To compare benign and metastatic lymph nodes, the Student t-test was employed. Multivariate logistic regression analyses were performed using texture parameters to identify independent predictors of metastatic lymph nodes. In order to address multicollinearity, variables highly associated with each other were excluded from the regression model using the backward stepwise analysis method. The impact of variables in the regression model was indicated by odds ratios (ORs). Receiver operating characteristic (ROC) curve analysis was conducted to evaluate the diagnostic performance of the univariate and multivariate texture parameters. During multivariate analysis, the area under the curve (AUC) values were calculated using the predictive values derived from the regression model. In this study, a significance level of 0.05 was utilized to determine statistical significance in all analyses.

#### Result

The study included 12 male (80%) and 3 female (20%) NPC patients with an average age of  $52.07 \pm 7.81$  years (range, 40–66 years). The healthy subjects included 23

male (76.7%) and 7 female (23.3%) with an average age of  $53.07 \pm 6.05$  years (range, 43–62 years). NPC group and healthy subjects did not differ in terms of age or gender ( $p > 0.05$ ). Finally, the study examined 32 metastatic lymph nodes and 30 benign lymph nodes (Figure 1).

Table 1 summarizes the mean and standard deviation of the texture parameters in groups with benign and metastatic lymph nodes. The first order texture features did not significantly differ between the groups ( $p > 0.05$ ). All GLCM features in metastatic lymph nodes were significantly different ( $p < 0.05$ ), with the exception of the correlation. Metastatic lymph nodes showed a significant difference in all GLRLM features ( $p < 0.05$ ).

The findings of the multivariate logistic regression analyses on texture parameters are presented in Table 2. Joint entropy, joint energy, and maximum probability were independent predictors of metastatic lymph nodes among the texture parameters obtained from GLCM features. Gray level non uniformity and low gray level run emphasis were independent predictors of metastatic lymph nodes among the texture parameters obtained from GLRLM features.

Table 3 displays the results of the ROC analysis for multivariate texture features for identifying metastatic lymph nodes. The AUC values for the GLCM regression model and GLRLM regression model were 0.975 and 0.928, respectively, and both demonstrated excellent diagnostic performance for identifying metastatic lymph nodes in NPC (Figure 2).

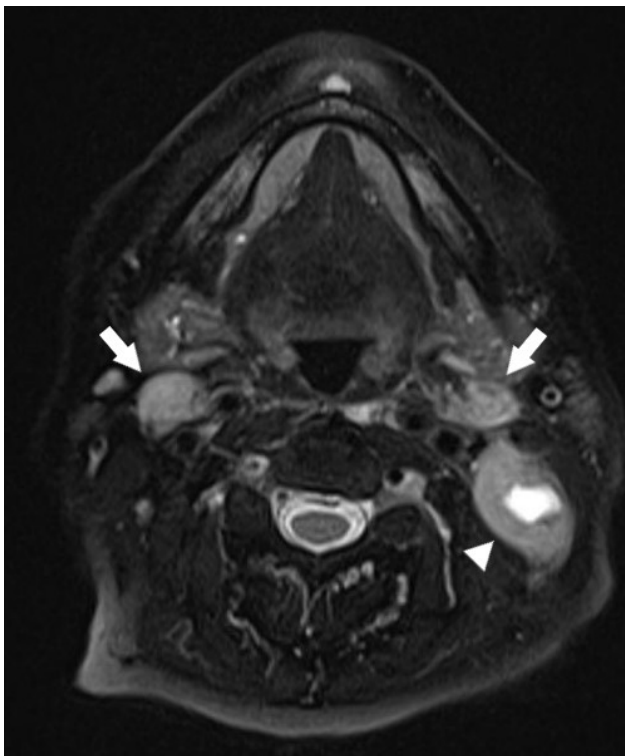


**Figure 1.** On axial postcontrast T1WI, there are level III lymphadenopathies on both sides (arrows and arrowhead). Lymphadenopathy on the left side has a cystic component (arrowhead).

**Table 1.** Texture parameters of benign and malign lymph nodes extracted from post contrast T1-weighted images.

|                              | Metastatic lymph nodes    | Benign lymph nodes         | p      |
|------------------------------|---------------------------|----------------------------|--------|
| <b>First order features</b>  |                           |                            |        |
| Entropy                      | $5.36 \pm 0.21$           | $5.22 \pm 0.35$            | 0.061  |
| Minimum                      | $898.25 \pm 625.69$       | $911.74 \pm 641.60$        | 0.933  |
| 10 <sup>th</sup> percentile  | $999.07 \pm 712.96$       | $1017.65 \pm 708.03$       | 0.918  |
| 90 <sup>th</sup> percentile  | $1178.57 \pm 855.34$      | $1282.37 \pm 878.62$       | 0.639  |
| Maximum                      | $1278.29 \pm 918.36$      | $1384.49 \pm 989.77$       | 0.663  |
| Mean                         | $1088.81 \pm 785.36$      | $1155.81 \pm 788.72$       | 0.739  |
| Median                       | $1088.87 \pm 787.98$      | $1161.43 \pm 786.23$       | 0.718  |
| Interquartile range          | $93.94 \pm 80.68$         | $141.65 \pm 112.50$        | 0.059  |
| Range                        | $379.76 \pm 305.55$       | $472.75 \pm 378.57$        | 0.290  |
| Mean absolute deviation      | $56.17 \pm 47.57$         | $82.82 \pm 62.98$          | 0.064  |
| Standard deviation           | $70.37 \pm 58.79$         | $102.23 \pm 77.21$         | 0.071  |
| Skewness                     | $0.009 \pm 0.366$         | $-0.195 \pm 0.481$         | 0.066  |
| Kurtosis                     | $3.12 \pm 0.72$           | $3.14 \pm 1.50$            | 0.940  |
| Variance                     | $8300.16 \pm 16039.31$    | $16213.92 \pm 30199.05$    | 0.199  |
| Uniformity                   | $0.030 \pm 0.004$         | $0.031 \pm 0.007$          | 0.288  |
| <b>GLCM features</b>         |                           |                            |        |
| Auto correlation             | $1188.62 \pm 281.63$      | $1445.17 \pm 388.98$       | 0.005  |
| Joint average                | $32.52 \pm 4.08$          | $35.75 \pm 5.53$           | 0.012  |
| Cluster prominence           | $821257.64 \pm 392361.98$ | $1183587.86 \pm 537235.09$ | 0.004  |
| Cluster tendency             | $523.15 \pm 169.99$       | $641.55 \pm 216.87$        | 0.019  |
| Contrast                     | $62.74 \pm 54.80$         | $90.34 \pm 46.91$          | 0.038  |
| Correlation                  | $0.795 \pm 0.133$         | $0.720 \pm 0.190$          | 0.074  |
| Difference average           | $5.75 \pm 2.41$           | $7.18 \pm 1.95$            | 0.013  |
| Difference entropy           | $3.73 \pm 0.26$           | $3.92 \pm 0.22$            | 0.002  |
| Difference variance          | $23.10 \pm 17.58$         | $32.22 \pm 14.47$          | 0.030  |
| Joint energy                 | $0.004 \pm 0.004$         | $0.008 \pm 0.003$          | <0.001 |
| Joint entropy                | $8.48 \pm 1.09$           | $7.21 \pm 0.58$            | <0.001 |
| Inverse difference moment    | $0.185 \pm 0.060$         | $0.143 \pm 0.042$          | 0.003  |
| Inverse difference           | $0.274 \pm 0.062$         | $0.232 \pm 0.045$          | 0.004  |
| Inverse variance             | $0.191 \pm 0.054$         | $0.143 \pm 0.037$          | <0.001 |
| Maximum probability          | $0.012 \pm 0.005$         | $0.020 \pm 0.006$          | <0.001 |
| Sum average                  | $65.03 \pm 8.16$          | $71.49 \pm 11.05$          | 0.012  |
| Sum entropy                  | $6.05 \pm 0.50$           | $5.59 \pm 0.47$            | <0.001 |
| <b>GLRLM features</b>        |                           |                            |        |
| Short run emphasis           | $0.954 \pm 0.020$         | $0.967 \pm 0.015$          | 0.005  |
| Long run emphasis            | $1.230 \pm 0.110$         | $1.163 \pm 0.083$          | 0.009  |
| Gray level non uniformity    | $11.53 \pm 8.36$          | $3.39 \pm 1.16$            | <0.001 |
| Run percentage               | $0.936 \pm 0.028$         | $0.953 \pm 0.021$          | 0.008  |
| Gray level variance          | $154.10 \pm 47.78$        | $203.76 \pm 58.27$         | 0.001  |
| Run variance                 | $0.085 \pm 0.044$         | $0.060 \pm 0.034$          | 0.014  |
| Run entropy                  | $5.62 \pm 0.29$           | $5.33 \pm 0.36$            | 0.001  |
| Low gray level run emphasis  | $0.011 \pm 0.010$         | $0.017 \pm 0.006$          | 0.003  |
| High gray level run emphasis | $1223.68 \pm 282.08$      | $1447.62 \pm 361.93$       | 0.008  |

† Independent Samples T-Test, data presented mean  $\pm$  standard deviation. GLCM- gray-level co-occurrence matrix, GLRLM- gray-level run length matrix.

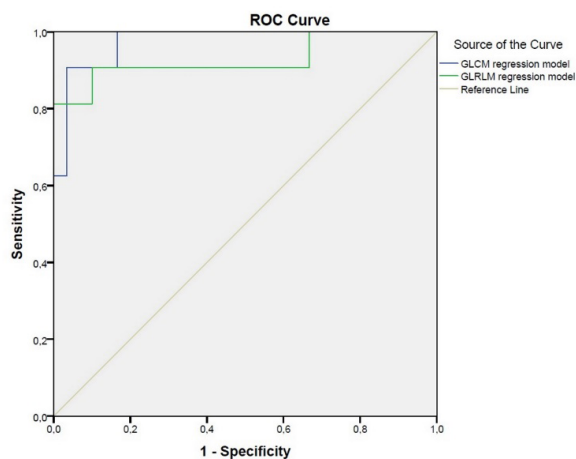


**Figure 2.** Receiver operating characteristic (ROC) curve of multivariate regression models to predict metastatic lymph nodes of patients with nasopharyngeal carcinoma.

**Table 2.** Multivariate logistic regression analyses for texture parameters extracted from post contrast T1- weighted images.

|                             | b       | S.E.   | Wald   | df | p     | Odds ratio | %95 CI |        |
|-----------------------------|---------|--------|--------|----|-------|------------|--------|--------|
|                             |         |        |        |    |       |            | Lower  | Upper  |
| <b>GLCM</b>                 |         |        |        |    |       |            |        |        |
| Joint entropy †             | 0.009   | 0.003  | 11.649 | 1  | 0.001 | 1.009      | 1.004  | 1.014  |
| Joint energy †              | 2.245   | 0.699  | 10.326 | 1  | 0.001 | 9.445      | 2.401  | 37.154 |
| Maximum probability †       | -0.569  | 0.245  | 5.419  | 1  | 0.020 | 0.566      | 0.350  | 0.914  |
| Constant                    | -70.596 | 20.852 | 11.462 | 1  | 0.001 | 0.000      |        |        |
| <b>GLRLM</b>                |         |        |        |    |       |            |        |        |
| Gray level non uniformity   | 1.853   | 0.567  | 10.664 | 1  | 0.001 | 6.377      | 2.098  | 19.389 |
| Low gray level run emphasis | 0.304   | 0.106  | 8.237  | 1  | 0.004 | 1.355      | 1.101  | 1.667  |
| Constant                    | -13.329 | 4.120  | 10.469 | 1  | 0.001 | 0.000      |        |        |

CI- confidence interval, GLCM- gray-level co-occurrence matrix, GLRLM- Gray-level run length matrix, † Odds ratio in units of 1000.

**Table 3.** ROC analysis results

|                        | AUC †                 | p      | Sensitivity (%) | Specificity (%) |
|------------------------|-----------------------|--------|-----------------|-----------------|
| GLCM regression model  | 0.975 (0.943 – 1)     | <0.001 | 90.6            | 96.7            |
| GLRLM regression model | 0.928 (0.857 – 0.999) | <0.001 | 90.6            | 90.0            |

† AUC- area under curve, GLCM- gray-level co-occurrence matrix, GLRLM- Gray-level run length matrix.

## Discussion

Metastatic lymph node detection and characterization are critical for treatment planning and prognosis in patients with NPC (1-3). Although MRI has emerged as a valuable tool for assessing lymph node status in NPC patients, current imaging methods are insufficient to distinguish between metastatic and non-metastatic lymph nodes (2, 4-9). Texture analysis based on MRI has shown promising results in improving the detection of metastatic lymph nodes in recent years (11-14,

17, 18). This study demonstrates that textural features extracted from MRI images can be used to distinguish between metastatic and non-metastatic neck lymph nodes of NPC.

The assessment of textural features within lymph nodes provides valuable information about tissue heterogeneity and cellular composition, which can be indicative of malignancy. Texture analysis involves the quantitative extraction of various parameters from radiological images, such as gray-level co-occurrence matrices, run-length matrices, and histogram-based measures. These parameters capture spatial variations in pixel intensities and provide insights into the underlying tissue architecture (10, 11).

Texture features derived from CT and MRI have been shown in studies to effectively distinguish between benign and metastatic lymph nodes in patients with head and neck squamous cancer (12, 13, 17-19). Texture analysis of MRI was shown to be a useful tool for nodal staging in head and neck squamous cell carcinoma in a study by Park et al. (12). Yuan et al. revealed that MRI texture analysis is a feasible tool for preoperative prediction of occult cervical node metastasis in early-stage oral squamous cell carcinoma (13). Kuno et al. demonstrated that texture features derived from CT can aid in the diagnosis of lymph node metastasis in HIV patients (14). In line with the literature, we demonstrated that MRI texture analysis helped with the diagnosis of lymph node metastasis in NPC.

Tomita et al. showed that combined texture features may provide helpful information for differentiating between nasopharyngeal cancer and nasopharyngeal lymphoma on unenhanced computed tomography (15). Zhao et al. demonstrated that MRI radiomics can predict treatment response and survival in patients with NPC (20). However, there is no TA research investigating the identification of lymph nodes in NPC patients in the literature.

Studies have shown that when compared to benign nodes, metastatic lymph nodes typically display higher entropy, greater heterogeneity, and more irregular patterns. These texture differences can be quantified and analyzed to improve the detection of lymph nodes (10-12). In our study, we observed that texture features indicating heterogeneity in metastatic lymph nodes were higher than in benign lymph nodes in NPC patients. The combination of texture analysis and conventional MRI evaluation has the potential to improve the diagnostic performance of lymph node assessment in NPC patients.

The small number of patients and the absence of pathological diagnosis of the lymph nodes are the methodological limitations of the study. Furthermore, it is critical to recognize the difficulties and limitations of TA. Standardization of MRI protocols and TA methods is critical for ensuring consistency and reproducibility across studies. The analysis algorithm and the ROI for TA can also have an impact on the results. Moreover, the impact of interobserver variability needs to be

addressed further addressed. In conclusion, MRI texture analysis may be useful to detect metastatic lymph nodes in patients with NPC by providing quantitative information on tissue heterogeneity and cellular composition. Continued research and validation are needed to establish the clinical utility of MRI texture analysis in the management of NPC patients.

### Author Contributions

Conception: H.Ö., Data Collection and Processing: N.Ö., Design: H.Ö., A.B., M.S.D., Supervision: A.B., A.K., Analysis and Interpretation: H.Ö., A.K., Literature Review: N.Ö., M.S.D., Writer: H.Ö., Critical Review: A.B., A.K.

### References

- Guo R, Mao Y-P, Tang L-L, Chen L, Sun Y, Ma J. The evolution of nasopharyngeal carcinomastaging. *Br J Radiol* 2019;92(1102):20190244.
- King AD. MR Imaging of Nasopharyngeal Carcinoma. *Magn Reson Imaging Clin N Am* 2022;30(1):19-33.
- Siti-Azrin AH, Norsa'adah B, Naing NN. Prognostic factors of nasopharyngeal carcinoma patients in a tertiary referral hospital: a retrospective cohort study. *BMC Res Notes* 2017;10(1):705.
- Abdel Khalek Abdel Razek A, King A. MRI and CT of nasopharyngeal carcinoma. *AJR Am J Roentgenol* 2012;198(1):11-8.
- Lan M, Huang Y, Chen CY, Han F, Wu SX, Tian L, et al. Prognostic Value of Cervical Nodal Necrosis in Nasopharyngeal Carcinoma: Analysis of 1800 Patients with Positive Cervical Nodal Metastasis at MR Imaging. *Radiology* 2015;276(2):536-44.
- Zhang GY, Liu LZ, Wei WH, Deng YM, Li YZ, Liu XW. Radiologic criteria of retropharyngeal lymph node metastasis in nasopharyngeal carcinoma treated with radiation therapy. *Radiology* 2010;255(2):605-12.
- Gupta A, Rahman K, Shahid M, Kumar A, Qaseem SM, Hassan SA, et al. Sonographic assessment of cervical lymphadenopathy: role of high-resolution and color Doppler imaging. *Head Neck* 2011;33(3):297-302.
- Ahuja AT, Ying M. Sonographic evaluation of cervical lymph nodes. *AJR Am J Roentgenol* 2005;184(5):1691-9.
- Wang XS, Hu CS, Ying HM, Zhou ZR, Ding JH, Feng Y. Patterns of retropharyngeal node metastasis in nasopharyngeal carcinoma. *Int J Radiat Oncol Biol Phys* 2009;73(1):194-201.
- Varghese BA, Cen SY, Hwang DH, Duddalwar VA. Texture Analysis of Imaging: What Radiologists Need to Know. *AJR Am J Roentgenol* 2019;212(3):520-8.
- Scheckenbach K, Colter L, Wagenmann M. Radiomics in Head and Neck Cancer: Extracting Valuable Information from Data beyond Recognition. *ORL J Otorhinolaryngol Relat Spec* 2017;79(1-2):65-71.
- Park JH, Bae YJ, Choi BS, Jung YH, Jeong W-J, Kim H, et al. Texture Analysis of Multi-Shot Echo-Planar Diffusion-Weighted Imaging in Head and Neck Squamous Cell Carcinoma: The Diagnostic Value for Nodal Metastasis. *J Clin Med* 2019;8(11):1767.
- Yuan Y, Ren J, Tao X. Machine learning-based MRI texture analysis to predict occult lymph node metastasis in early-stage oral tongue squamous cell carcinoma. *Eur Radiol* 2021;31(9):6429-37.
- Kuno H, Garg N, Qureshi MM, Chapman MN, Li B, Meibom SK, et al. CT Texture Analysis of Cervical Lymph Nodes on Contrast-Enhanced [18F] FDG-PET/CT Images to Differentiate Nodal Metastases from Reactive Lymphadenopathy in HIV-Positive Patients with Head and Neck Squamous Cell Carcinoma. *AJNR Am J Neuroradiol* 2019;40(3):543-50.
- Tomita H, Yamashiro T, Iida G, Tsubakimoto M, Mimura H, Murayama S. Unenhanced CT texture analysis with machine learning for differentiating between nasopharyngeal cancer and nasopharyngeal malignant lymphoma. *Nagoya J Med Sci* 2021;83(1):135-49.
- Liu L, Pei W, Liao H, Wang Q, Gu D, Liu L, et al. A Clinical-Radiomics Nomogram Based on Magnetic Resonance Imaging for Predicting Progression-Free Survival After Induction Chemotherapy in Nasopharyngeal Carcinoma. *Front Oncol* 2022;12:792535.
- Tomita H, Yamashiro T, Heianna J, Nakasone T, Kimura Y, Mimura H, et al. Nodal-based radiomics analysis for identifying cervical lymph node metastasis at levels I and II in patients with oral squamous cell carcinoma using contrast-enhanced computed tomography. *Eur Radiol* 2021;31(10):7440-9.
- Forghani R, Chatterjee A, Reinhold C, Pérez-Lara A, Romero-Sanchez G, Ueno Y, et al. Head and neck squamous cell carcinoma: prediction of cervical lymph node metastasis by dual-energy CT texture analysis with machine learning. *Eur Radiol* 2019;29(11):6172-81.
- Lu S, Ling H, Chen J, Tan L, Gao Y, Li H, et al. MRI-based radiomics analysis for preoperative evaluation of lymph node metastasis in hypopharyngeal squamous cell carcinoma. *Front Oncol* 2022;12:936040.
- Zhao L, Gong J, Xi Y, Xu M, Li C, Kang X, et al. MRI-based radiomics nomogram may predict the response to induction chemotherapy and survival in locally advanced nasopharyngeal carcinoma. *Eur Radiol* 2020;30(1):537-46.